Generalized Approach for Modeling Minimally Invasive Surgery as a Stochastic Process Using a Discrete Markov Model

Jacob Rosen*, *Member, IEEE*, Jeffrey D. Brown, Lily Chang, Mika N. Sinanan, and Blake Hannaford, *Fellow, IEEE*

***Abstract*—Minimally invasive surgery (MIS) involves a multidimensional series of tasks requiring a synthesis between visual information and the kinematics and dynamics of the surgical tools. Analysis of these sources of information is a key step in defining objective criteria for characterizing surgical performance. The Blue DRAGON is a new system for acquiring the kinematics and the dynamics of two endoscopic tools synchronized with the endoscopic view of the surgical scene. Modeling the process of MIS using a finite state model [Markov model (MM)] reveals the internal structure of the surgical task and is utilized as one of the key steps in objectively assessing surgical performance. The experimental protocol includes tying an intracorporeal knot in a MIS setup performed on an animal model (pig) by 30 surgeons at different levels of training including expert surgeons. An objective learning curve was defined based on measuring quantitative statistical distance (similarity) between MM of experts and MM of residents at different levels of training. The objective learning curve was similar to that of the subjective performance analysis. The MM proved to be a powerful and compact mathematical model for decomposing a complex task such as laparoscopic suturing. Systems like surgical robots or virtual reality simulators in which the kinematics and the dynamics of the surgical tool are inherently measured may benefit from incorporation of the proposed methodology.**

***Index Terms*—Dynamics, haptics, human machine interface, kinematics, manipulation, Markov model, minimally invasive, robotics, simulation, soft tissue, surgery, surgical skill assessment, surgical tool, vector quantization.**

I. Introduction

EVALUATION of procedural skills in surgery can be performed utilizing three different modalities: during actual open or minimally invasive clinical procedures; in physical or virtual reality simulators with or without haptic feedback; and during interaction with surgical robotic systems (Fig. 1). During open or minimally invasive surgical (MIS) procedures, the surgeon interacts with the patient's tissue either directly with his/her hands or through the mediation of tools. Surgical robotic enables the surgeon to operate in a teleoperation mode with or without force feedback using a master/slave system configuration. In this mode of operation, visualization is obtained from either an external camera or an endoscopic camera. Incorporating force feedback allows the surgeon to feel through the master console the forces being applied on the tissue by the surgical robot, the slave, as he/she interacts with it from the master console. The surgical tools, the robot–slave, and the anatomical structures are replaced with virtual counterparts for training in a simulated virtual environment. The surgeon interacts with specially designed input devices, haptic devices when force feedback is incorporated, that emulate surgical tools, or with the master console of the robotic system itself, and performs surgical procedures in virtual reality.

One element that all of these modalities have in common is the human-machine interface in which visual, kinematic, dynamic, and haptic information is shared. This interface, rich with multidimensional data, is a valuable source of objective information that can be used to objectively assess technical surgical and medical skill within the general framework of surgical and medical ability. Algorithms that are developed for objective assessment of skill are independent of the modality being used, and therefore, the same algorithms can be incorporated into any of these technologies.

As the medical profession is faced with demands for greater accountability and patient safety, there is a critical need for the development of consistent and reliable methods for objective evaluation of clinician performance during procedures. The methodology for assessing surgical skill as a subset of surgical ability [1], [2], is gradually shifting from subjective scoring by an expert which may be a variably biased opinion using vague criteria, toward a more objective, quantitative analysis. This shift is enabled by using instrumented tools [3]–[6], measurements of the surgeon's arm kinematics [7], gaze patterns [8], physical simulators [9], a variety of virtual reality simulators with and without haptics [1], [10], and robotic systems [11]. Regardless of the modality being used or the clinical procedure being studied, task deconstruction or decomposition is an essential component of a rigorous objective skills-assessment methodology. A broader understanding of procedures is achieved by exposing and analyzing the internal hierarchy of tasks while providing objective means for quantifying training and skills acquisition.

Manuscript received December 20, 2004; revised June 11, 2005. This work was supported in part by a major grant from US Surgical, a division of Tyco, Inc. to the University of Washington, Center for Videoendoscopic Surgery and inpart by a gift from Washington Research Foundation Capital. *Asterisk indicates corresponding author.*

*J. Rosen is with the Department of Electrical Engineering, University of Washington, Box 352500, Seattle WA 98195-2500 USA (e-mail: rosen@u.washington.edu; URL: Biorobotics Lab: http://brl.ee.washington.edu; Center of Videoendoscopic Surgery: http://depts.washington.edu/cves/).

J. D. Brown is with the Department of Bioengineering, University of Washington, Seattle WA 98195-2500 USA (e-mail: jdbrown@u.washington.edu).

L. Chang and M. Sinanan are with the Department of Surgery, University of Washington, Seattle WA 98195-2500 USA (e-mail: lchang@u.washington.edu; mssurg@u.washington.edu).

B. Hannaford is with the Department of Electrical Engineering, University of Washington, Seattle WA 98195-2500 USA (e-mail: blake@u.washington.edu).

Digital Object Identifier 10.1109/TBME.2005.869771

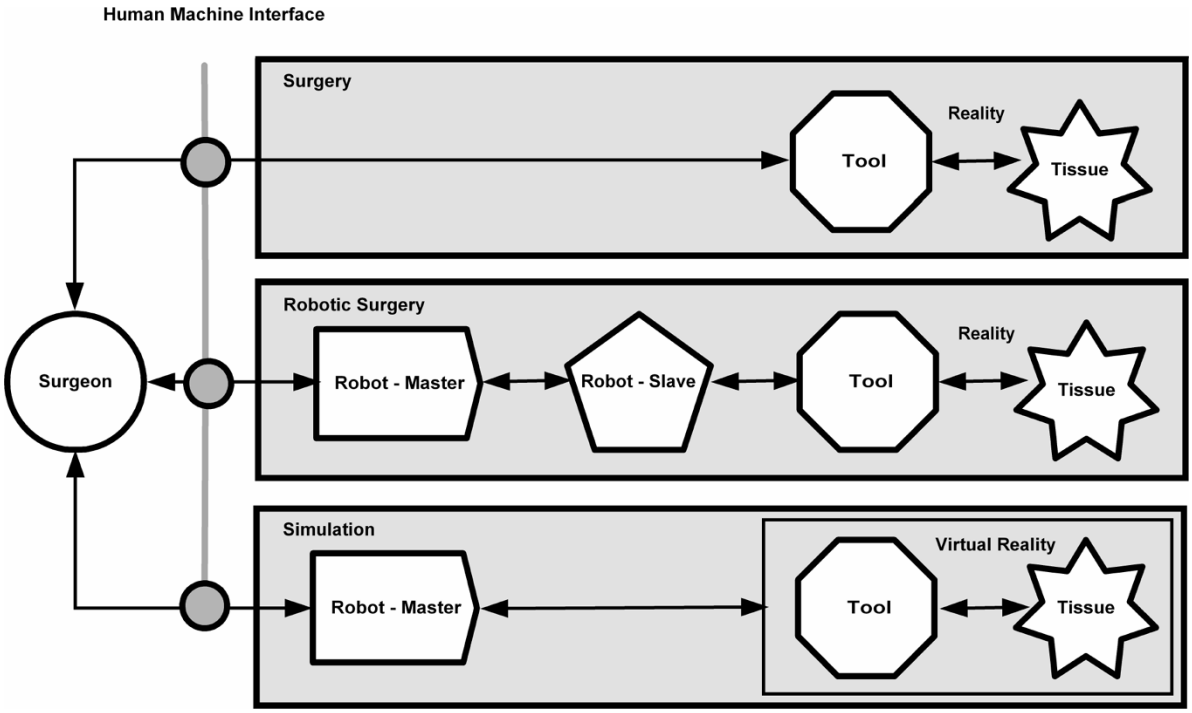

Fig. 1. Modalities for performing surgery.

Task decomposition is associated with defining the prime elements of the process. In surgery, a procedure is methodologically divided into steps, stages, or phases with well-defined intermediate goals. Additional hierarchical decomposition is based upon identifying tasks or subtasks [12] composed of sequence of and actions or states [3]–[6]. In addition, other measurable parameters such as workspace [13] completion time, tool position, and forces and torques were studied individually [3]–[6]. Selecting low-level elements of the task decomposition allows one to associate these elements with quantifiable and measurable parameters. The definition of these states, along with measurable, quantitative data, are the foundation for modeling and examining surgical tasks as a process. Markov Modeling (MM) and its subset, Hidden Markov Modeling (HMM), were extensively developed in the area of speech recognition [14] and further used in a broad spectrum of other fields, e.g., gesture recognition and facial expressions [15], [16] DNA and protein modeling [17], surgical tools in MIS setup [4], [18], and teleoperation [19]–[23].

The current study is different from our earlier work [3]–[6] in terms of: 1) the size of the subject pool—30 subjects as opposed to 10; 2) the spectrum of skill levels—full spectrum including 6 different training levels (each year of the 5 years of residency training and an expert level) as opposed to a discrete spectrum; 3) the experimental system and the data stream—the Blue DRAGON monitoring 26 channels including position/orientation, forces/torque, and contact signals from two surgical tools as opposed to 7 force/torque measurements acquired by a single tool; 4) the nature of the surgical task—specific fundamental task such as suturing as opposed to steps of a MIS procedure; 5) Type of model—30 state Markov model (MM) representing two tools working collaboratively as opposed to 3 and 15 state Hidden Markov Models (HMM) representing one tool; 6) Complementary analysis—comparison with a subjective expert evaluation as well as tool path and completion time.

The specific aim of the current study was to develop a system for acquiring data in a real MIS setup using an animal model and a methodology for decomposing two-handed surgical tasks using MMs based on the kinematics and the dynamics of the surgical tools. Measuring the statistical similarity between the models representing subjects at different levels of their surgical training enables an objective assessment of surgical skill.

II. Tools and Methods

A novel system named the Blue DRAGON was designed, constructed, and used for acquiring the kinematics (position and orientation) and the dynamics (force and torque) of two endoscopic tools during MIS procedures in real-time. The data were acquired during a surgical task performed by 30 subjects at different levels of surgical training followed by objective and subjective surgical skill analysis based on task decomposition. The novel objective methodology was based upon a multistate MM whereas the subjective methodology utilized a standard scoring system for analyzing the videotapes of the surgical scene recorded during the experiment. The following subsections describe the system and the methodologies that were used in the current study.

A. Tools—The Blue DRAGON System

The Blue DRAGON is a system for acquiring the kinematics and the dynamics of two endoscopic tools along with the endoscopic view of the surgical scene while performing a MIS procedure (Fig. 2). The system includes two four-bar passive mechanisms attached to endoscopic tools [5]. The endoscopic tool in MIS is inserted into the body through a port located, for example, in the abdominal wall. The tool is rotated around a pivot point within the port that is inaccessible to sensors measuring the tool's rotation. The four bar mechanism is one of several mechanisms that allows mapping of the tool's rotation around the port's pivot point. This mapping is enabled by aligning the

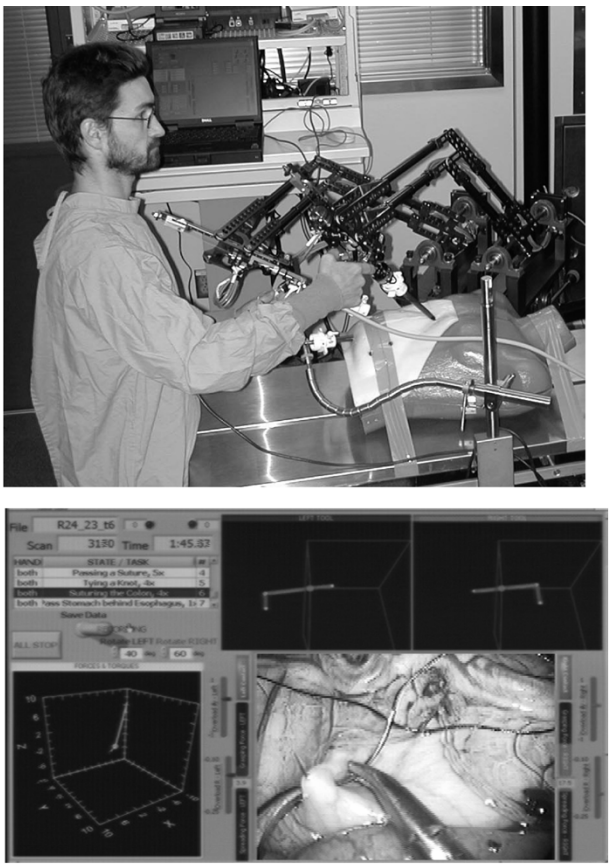

Fig. 2. The Blue DRAGON system (a) the system integrated into a MIS operating room (b) graphical user interface.

remote rotational center with the pivot point of the endoscopic tool located inside the port. The tool's positions and orientations, with respect to the port, are then tracked by sensors that are incorporated into the mechanism's joints. This setup makes the mechanism totally transparent to the moments that are generated intentionally by using the tools. The two mechanisms are equipped with three classes of sensors: 1) position sensors (potentiometers—Midori America Corp.) are incorporated into four of the mechanism's joints for measuring the position, orientation, and translation of the two instrumented endoscopic tools attached to them. In addition, two linear potentiometers (Penny & Giles Controls Ltd.) that are attached to the tools' handles are used for measuring the endoscopic handle and tool tip angles; 2) three-axis force/torque (F/T) sensors with holes drilled at their center (ATI-Mini sensor) are inserted and clamped to the proximal end of the endoscopic tools' shafts. In addition, double beam force sensors (Futak) were inserted into the tools' handles for measuring the grasping forces at the hand/tool interface; 3) contact sensors, based on RC circuit, provided binary indication of any tool-tip/tissue contact.

Data measured by the Blue DRAGON sensors are acquired using two 12-bit USB A/D cards (National Instruments) sampling the 26 channels (4 rotations, 1 translation, 1 tissue contact, and 7 channels of forces and torques from each instrument including grasper) at 30 Hz. Preliminary tests acquiring data at a sampling rate of 1 KHz indicated that 95% of the signals' accumulated energy is in a bandwidth 0–5 Hz. In addition, a graphical user interface (GUI) [Fig. 2(b)] displayed information measured by the Blue DRAGONs in real-time while incorporating the endoscopic view of the surgical scene acquired by the endoscope's video camera. On the top right side of the GUI, a virtual representation of the two endoscopic tools are shown along with vectors representing the instantaneous velocities. On the bottom left, a three-dimensional representation of the forces and torque vectors is presented. Surrounding the endoscopic image are bars representing the grasping/spreading forces applied on the handle and transmitted to the tool tip via the tool's internal mechanism, along with virtual binary LEDs indicating contact between the tool tips and the tissues.

B. Experimental Protocol

The experimental protocol included 30 surgeons at different levels of expertise from surgeons in training to surgical attendings skilled in laparoscopic surgery. There were five subjects in each group representing the five years of surgical training ($5 \times$ R1, R2, R3, R4, R5—where the numeral denotes year of training) and five expert surgeons. For the purpose of this study an expert surgeon (E) was defined as a board certified surgeon who has performed at least 800 proceedures and practices medicine as an attending physician. Each subject was given instruction on how to perform an intracorporeal knot through a standard multimedia presentation. The multimedia presentation included a written description of the task along with a video clip of the surgical scene and audio explanation of the task. None of the subjects, included in this study, had any prior experience performing surgery with the Blue DRAGON. Each surgeon was given a 5-min unsupervised time segment to familiarize herself/himself with the system prior to the experiment. Subjects were then given a maximum of 15 min to complete this task in a swine model. This complex, integrative task includes many of the elements of advanced MIS techniques. An expert surgeon reviewed all the videotapes recorded during the experiment and verified that all the subjects followed the steps specified in the instruction.

In addition to the surgical task, all the subjects (30 surgeons) performed 15 predefined tool/tissue and tool/needle-suture interactions during a time interval of 1 min each. The kinematics (the position/orientation of the tools in space with respect to the port) and the dynamics (forces and torque F/T applied by the surgeons on the tools) of the left and right endoscopic tools along with the visual view of the surgical scene were acquired by a passive mechanism that is part of the Blue DRAGON. The aim of this experimental segment was to study the F/T and velocity signatures associated with each interaction that were further used as the model observations associated with each state of the model. All animal procedures were performed in an AALAC-accredited surgical research facility under an approved protocol from the institutional animal care committee of the University of Washington.

C. Objective Analysis—MIS Task Decomposition and Markov Model

1) Surgery as a Language—The Analogy and the State Definitions: The objective methodology for assessing skill while performing a procedure is inspired by the analogy between the human spoken language and surgery. Further analysis of this concept indicates that these two domains share similar

TABLE I
THE ANALOGY BETWEEN THE HUMAN SPOKEN LANGUAGE AND SURGERY AS MANIFESTED ITSELF IN A SIMILAR TAXONOMY AND SUB STRUCTURES ALONG WITH THE CORRESPONDING ELEMENT OF THE FINITE STATE MARKOV MODEL

Language	Surgery	Model
Story	Operation / Procedure	Multiple Models
Chapter	Step of the Operation	Model
Word	Tool/Tissue Interaction	State
Pronunciation	Force Torque Velocity magnitude	Observation

taxonomy and internal etymological structure that allows a mathematical description of the process by using quantitative models. Such models can be further used to objectively assess skill level by revealing the internal structure and dynamics of the process. This analogy is enhanced by the fact that in both the human language and in surgery, an idea can be expressed and a procedure can be performed in several different ways while retaining the same cognitive meaning or outcome. This fact suggests that a stochastic approach might describe the surgical or medical examination processes incorporating the inherent variability better then a deterministic approach.

Table I summarizes the analogy between the two entities, human language and surgery, along with the corresponding modeling elements in a hierarchal fashion. The critical step in creating such an analogy is to identify the prime elements. In the human language, the prime element is the "word" which is analogous to a "tool/tissue interaction" in surgery. This prime element is modeled by a "state" in the model. As in a spoken language, words can have different "pronunciations" by various people and yet preserve their meaning. In surgery, various "force/torque magnitudes" can be applied on the tissues and still be classified under the same tool/tissue interaction category. These various force/torque magnitudes are simulated by the "observations" in the model. In a similar fashion to the human language in which a sequence of words comprise a sentence, and sentences create a "chapter," a sequence of tool/tissue interactions form a step of an operation in which an intermediate and specific outcome can be completed. Each step of the operation is represented by a single model. "Multiple models" can be further described as a multistep "surgical operation" that is analogous to a "story." One may note that the substructures like "sentence" and a "paragraph" were omitted in the current analogy; however, identifying the corresponding elements in surgical procedure may increase the resolution of the model.

Analyzing the degrees of freedom (DOFs) of a tool in MIS indicates that due to the introduction of the port through which the surgeon inserts tools into the body cavity, two DOF of the tool are restricted. The six DOF of a typical open surgical tool is reduced to only four DOF in a minimally invasive setup (Fig. 3). These four DOF include rotation along the three orthogonal axes (x, y, z) and translation along the long axis of the tool's shaft (z). A fifth DOF is defined as the tool-tip jaws angle, which is mechanically linked to the tool's handle, when a grasper or a scissor is used. Additional one or two DOFs can be obtained by adding a wrist joint to the MIS tool. The wrist joint has been incorporated into commercially available surgical robots in order to enhance the dexterity of the tool within the body cavity.

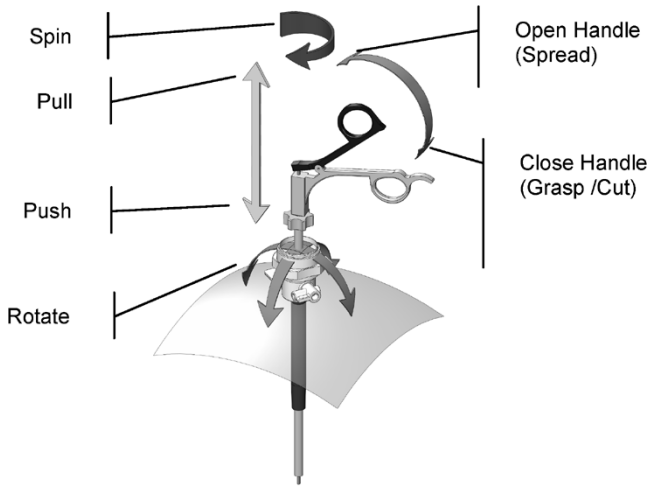

Fig. 3. Definition of the five DOFs (marked by arrows) of a typical MIS endoscopic tool. Note that two DOF were separated into two distinct actions (Open/Close handle and Pull/Push), and the other two were lumped into one action (Rotate) for representing the tool tip tissue interactions (omitted in the illustration). The terminology associated with the various DOF corresponds with the model state definitions (Table II).

Surgeons, while performing MIS procedures, utilize various combinations of the tools' DOF while manipulating them during the interaction with the tissues or other items in the surgical scene (needle, suture, staple etc.) in order to achieve the desired outcome. Quantitative analysis of the tool's position and orientation during surgical procedures revealed 15 different combinations of the tool's five DOF which will be further referred to and modeled as states (Table II). The 15 states can be grouped into three types, based on the number of movements or DOF utilized simultaneously. The fundamental maneuvers are defined as Type I. The "idle" state was defined as moving the tool in space (body cavity) without touching any internal organ, tissue, or any other item in the scene. The forces and torques developed in this state represent the interaction with the port and the abdominal wall, in addition to the gravitational and inertial forces. In the "grasping" and "spreading" states, compression and tension were applied on the tissue through the tool tip by closing and opening the grasper's handle, respectively. In the "pushing" state, the tissue was compressed by moving the tool along the Z axis. "Sweeping" consisted of placing the tool in one position while rotating it around the X and/or Y axes or in any combination of these two axes (port frame). The rest of the tool/tissue interactions, Types II and III, were combinations of the fundamental ones defined as Type I. The only one exception was state 15 that was observed only in tasks involving suturing when the surgeon grasps the needle and rotates it around the shaft's long axis to insert it into the tissue. Such a rotation was never observed whenever direct tissue interaction was involved.

2) Vector Quantization (VQ): Each one of the 15 states was associated with a unique set of forces, torques, and angular and linear velocities, as indicated in Table II. Following the language analogy, in the same way that a word correlates to a state that may be pronounced differently and still retains the same meaning, the tool might be in a specific state while infinite combinations of forces, torques, and angular and linear velocities may be used. A significant data reduction was achieved by using a clustering analysis in a search for a discrete number of high

TABLE II

DEFINITIONS OF THE 15 STATES BASED ON SPHERICAL COORDINATE SYSTEM WITH AN ORIGIN AT THE PORT. EACH STATE IS CHARACTERIZED BY A UNIQUE SET OF ANGULAR/LINEAR VELOCITIES, FORCES AND TORQUES AND ASSOCIATED WITH A SPECIFIC TOOL/TISSUE OR TOOL/OBJECT INTERACTION. A NON-ZERO THRESHOLD VALUE IS DEFINED FOR EACH PARAMETER BY ε. THE STATES' DEFINITIONS ARE INDEPENDENT FROM THE TOOL TIP BEING USED, e.g., THE STATE DEFINED AS CLOSING HANDLE MIGHT BE ASSOCIATED WITH GRASPING OR CUTTING IF A GRASPER OR SCISSORS ARE BEING USED, RESPECTIVELY

Type	No.	State Name	State Acronym	Tissue Contact	Position / Orientation					Force / Torque						
					ω_x	ω_y	ω_z	v_r	ω_g	F_x	F_y	F_z	T_x	T_y	T_z	F_g
I	1	Idle	ID	-	$\pm\varepsilon_{\omega_x}$	$\pm\varepsilon_{\omega_y}$	$\pm\varepsilon_{\omega_z}$	$\pm\varepsilon_{v_r}$	$\pm\varepsilon_{\omega_g}$	$\pm\varepsilon_{F_x}$	$\pm\varepsilon_{F_y}$	$\pm\varepsilon_{F_z}$	$\pm\varepsilon_{T_x}$	$\pm\varepsilon_{T_y}$	$\pm\varepsilon_{T_z}$	$\pm\varepsilon_{F_g}$
	2	Closing Handle (Grasping)	CL	+	$\pm\varepsilon_{\omega_x}$	$\pm\varepsilon_{\omega_y}$	$\pm\varepsilon_{\omega_z}$	$\pm\varepsilon_{v_r}$	$\omega_g < \varepsilon_{\omega_g}$	$\pm\varepsilon_{F_x}$	$\pm\varepsilon_{F_y}$	$\pm\varepsilon_{F_z}$	$\pm\varepsilon_{T_x}$	$\pm\varepsilon_{T_y}$	$\pm\varepsilon_{T_z}$	$F_g > \varepsilon_{F_g}$
	3	Opening Handle (Spreading)	OP	+	$\pm\varepsilon_{\omega_x}$	$\pm\varepsilon_{\omega_y}$	$\pm\varepsilon_{\omega_z}$	$\pm\varepsilon_{v_r}$	$\omega_g > \varepsilon_{\omega_g}$	$\pm\varepsilon_{F_x}$	$\pm\varepsilon_{F_y}$	$\pm\varepsilon_{F_z}$	$\pm\varepsilon_{T_x}$	$\pm\varepsilon_{T_y}$	$\pm\varepsilon_{T_z}$	$F_g < -\varepsilon_{F_g}$
	4	Pushing	PS	+	$\pm\varepsilon_{\omega_x}$	$\pm\varepsilon_{\omega_y}$	$\pm\varepsilon_{\omega_z}$	$v_r < -\varepsilon_{v_r}$	$\pm\varepsilon_{\omega_g}$	$\pm\varepsilon_{F_x}$	$\pm\varepsilon_{F_y}$	$F_z > \varepsilon_{F_z}$	$\pm\varepsilon_{T_x}$	$\pm\varepsilon_{T_y}$	$\pm\varepsilon_{T_z}$	$\pm\varepsilon_{F_g}$
	5	Rotating (Sweeping)	RT	+	$\omega_x > \lvert\varepsilon_{\omega_x}\rvert$	$\omega_y > \lvert\varepsilon_{\omega_y}\rvert$	$\pm\varepsilon_{\omega_z}$	$\pm\varepsilon_{v_r}$	$\pm\varepsilon_{\omega_g}$	$F_x > \lvert\varepsilon_{F_x}\rvert$	$F_y > \lvert\varepsilon_{F_y}\rvert$	$\pm\varepsilon_{F_z}$	$T_x > \lvert\varepsilon_{T_x}\rvert$	$T_y > \lvert\varepsilon_{T_y}\rvert$	$\pm\varepsilon_{T_z}$	$\pm\varepsilon_{F_g}$
II	6	Closing - Pulling	CL -PL	+	$\pm\varepsilon_{\omega_x}$	$\pm\varepsilon_{\omega_y}$	$\pm\varepsilon_{\omega_z}$	$v_r > \varepsilon_{v_r}$	$\omega_g < \varepsilon_{\omega_g}$	$\pm\varepsilon_{F_x}$	$\pm\varepsilon_{F_y}$	$F_z < -\varepsilon_{F_z}$	$\pm\varepsilon_{T_x}$	$\pm\varepsilon_{T_y}$	$\pm\varepsilon_{T_z}$	$F_g > \varepsilon_{F_g}$
	7	Closing - Pushing	CL -PS	+	$\pm\varepsilon_{\omega_x}$	$\pm\varepsilon_{\omega_y}$	$\pm\varepsilon_{\omega_z}$	$v_r < -\varepsilon_{v_r}$	$\omega_g < \varepsilon_{\omega_g}$	$\pm\varepsilon_{F_x}$	$\pm\varepsilon_{F_y}$	$F_z > \varepsilon_{F_z}$	$\pm\varepsilon_{T_x}$	$\pm\varepsilon_{T_y}$	$\pm\varepsilon_{T_z}$	$F_g > \varepsilon_{F_g}$
	8	Closing - Rotating	CL-RT	+	$\omega_x > \lvert\varepsilon_{\omega_x}\rvert$	$\omega_y > \lvert\varepsilon_{\omega_y}\rvert$	$\pm\varepsilon_{\omega_z}$	$\pm\varepsilon_{v_r}$	$\omega_g < \varepsilon_{\omega_g}$	$F_x > \lvert\varepsilon_{F_x}\rvert$	$F_y > \lvert\varepsilon_{F_y}\rvert$	$\pm\varepsilon_{F_z}$	$\pm\varepsilon_{T_x}$	$\pm\varepsilon_{T_y}$	$\pm\varepsilon_{T_z}$	$F_g > \varepsilon_{F_g}$
	9	Pushing - Opening	PS-OP	+	$\pm\varepsilon_{\omega_x}$	$+\varepsilon_{\omega_y}$	$\pm\varepsilon_{\omega_z}$	$v_r < -\varepsilon_{v_r}$	$\omega_g > \varepsilon_{\omega_g}$	$\pm\varepsilon_{F_x}$	$+\varepsilon_{F_y}$	$F_z < -\varepsilon_{F_z}$	$\pm\varepsilon_{T_x}$	$+\varepsilon_{T_y}$	$\pm\varepsilon_{T_z}$	$F_g < -\varepsilon_{F_g}$
	10	Pushing - Rotating	PS-RT	+	$\omega_x > \lvert\varepsilon_{\omega_x}\rvert$	$\omega_y > \lvert\varepsilon_{\omega_y}\rvert$	$\pm\varepsilon_{\omega_z}$	$v_r < -\varepsilon_{v_r}$	$+\varepsilon_{\omega_g}$	$F_x > \lvert\varepsilon_{F_x}\rvert$	$F_y > \lvert\varepsilon_{F_y}\rvert$	$F_z > \varepsilon_{F_z}$	$\pm\varepsilon_{T_x}$	$\pm\varepsilon_{T_y}$	$\pm\varepsilon_{T_z}$	$\pm\varepsilon_{F_g}$
	11	Rotating - Opening	RT-OP	+	$\omega_x > \lvert\varepsilon_{\omega_x}\rvert$	$\omega_y > \lvert\varepsilon_{\omega_y}\rvert$	$\pm\varepsilon_{\omega_z}$	$\pm\varepsilon_{v_r}$	$\omega_g > \varepsilon_{\omega_g}$	$F_x > \lvert\varepsilon_{F_x}\rvert$	$F_y > \lvert\varepsilon_{F_y}\rvert$	$\pm\varepsilon_{F_z}$	$T_x > \lvert\varepsilon_{T_x}\rvert$	$T_y > \lvert\varepsilon_{T_y}\rvert$	$\pm\varepsilon_{T_z}$	$F_g < -\varepsilon_{F_g}$
III	12	Closing - Pulling - Rotating	CL-PL-RT	+	$\omega_x > \lvert\varepsilon_{\omega_x}\rvert$	$\omega_y > \lvert\varepsilon_{\omega_y}\rvert$	$\pm\varepsilon_{\omega_z}$	$v_r > \varepsilon_{v_r}$	$\omega_g < \varepsilon_{\omega_g}$	$F_x > \lvert\varepsilon_{F_x}\rvert$	$F_y > \lvert\varepsilon_{F_y}\rvert$	$F_z < -\varepsilon_{F_z}$	$\pm\varepsilon_{T_x}$	$\pm\varepsilon_{T_y}$	$\pm\varepsilon_{T_z}$	$F_g > \varepsilon_{F_g}$
	13	Closing -Pushing - Rotating	CL-PS-	+	$\omega_x > \lvert\varepsilon_{\omega_x}\rvert$	$\omega_y > \lvert\varepsilon_{\omega_y}\rvert$	$\pm\varepsilon_{\omega_z}$	$v_r < -\varepsilon_{v_r}$	$\omega_g < \varepsilon_{\omega_g}$	$F_x > \lvert\varepsilon_{F_x}\rvert$	$F_y > \lvert\varepsilon_{F_y}\rvert$	$F_z > \varepsilon_{F_z}$	$T_x > \lvert\varepsilon_{T_x}\rvert$	$T_y > \lvert\varepsilon_{T_y}\rvert$	$\pm\varepsilon_{T_z}$	$F_g > \varepsilon_{F_g}$
	14	Pushing - Rotating - Opening	PS-RT-	+	$\omega_x > \lvert\varepsilon_{\omega_x}\rvert$	$\omega_y > \lvert\varepsilon_{\omega_y}\rvert$	$\pm\varepsilon_{\omega_z}$	$v_r < -\varepsilon_{v_r}$	$\omega_g > \varepsilon_{\omega_g}$	$F_x > \lvert\varepsilon_{F_x}\rvert$	$F_y > \lvert\varepsilon_{F_y}\rvert$	$F_z > \varepsilon_{F_z}$	$\pm\varepsilon_{T_x}$	$\pm\varepsilon_{T_y}$	$\pm\varepsilon_{T_z}$	$F_g < -\varepsilon_{F_g}$
II	15	Closing Handle - Spinning	CL-SP	+	$\pm\varepsilon_{\omega_x}$	$\pm\varepsilon_{\omega_y}$	$\lvert\omega_z > \varepsilon_{\omega_z}\rvert$	$\pm\varepsilon_{v_r}$	$\omega_g < \varepsilon_{\omega_g}$	$\pm\varepsilon_{F_x}$	$\pm\varepsilon_{F_y}$	$\pm\varepsilon_{F_z}$	$\pm\varepsilon_{T_x}$	$\pm\varepsilon_{T_y}$	$T_z > \lvert\varepsilon_{T_z}\rvert$	$F_g > \varepsilon_{F_g}$

concentration cluster centers in the database for each one of the 15 states. As part of this process, the continuous 13-dimensional (13-D) vectors were transformed into one-dimensional vectors of 150 symbols (10 symbols for each state that was determined by the error distortion criterion).

The data reduction was performed in three phases. During the first phase a subset of the database was created by appending all the 13-D vectors associated with each state measured by the left and the right tools and performed by all the subjects (see Section II-B for details). The 13-D subset of the database (ω_x, ω_y, ω_z, ω_g, V_Z, F_x, F_y, F_z, T_x, T_y, T_z, F_g, U) was transformed into a nine-dimensional vector $\overline{X}_i = [\omega_{xy}, \omega_z, \omega_g, V_Z, F_{xy}, F_z, T_{xy}, T_z, F_g]$ by calculating the magnitude of the angular velocity, forces, and torques in the XY plane ($\omega_{xy} = \sqrt{\omega_x^2 + \omega_y^2}$, $F_{xy} = \sqrt{F_x^2 + F_y^2}$, $T_{xy} = \sqrt{T_x^2 + T_y^2}$). This process canceled out differences between surgeons due to variations in position relative to the animal and allowed the use of the same clusters for the left and the right tools. Note the tenth dimension U was omitted. This variable used to differentiate the Idle state (State 1) in which the tool tip is not in contact with the tissue or other elements in the scene out of all the other states (States 2–15).

The subscripts x, y, z are use to associate the angular and linear velocities (ω, V), forces (F), and torques (T) with the stationary coordinate system and an origin located at the surgical port. The combined axes x-y, x-z, and y-z define planes parallel to the coronal, sagittal, and transverse planes, respectively. The Z axis is pointing toward the anterior side of the abdominal wall. The subscript g is used to associate the angular velocities (ω) and the forces (F) with the tool's grasping handle. The binary variable U indicates whether the tool is in contact with the tissue or any other element in the surgical scene.

As part of the second phase, a K-means vector quantization algorithm [24] was used to identify 10 cluster centers associated with each state. Given M patterns $\overline{X}_1, \overline{X}_2, \ldots, \overline{X}_M$ contained in the pattern space $\overline{S}$, the process of clustering can be formally stated as seeking the regions $\overline{S}_1, \overline{S}_2, \ldots, \overline{S}_K$ such that every data vector $\overline{X}_i$ $(i = 1, 2, \ldots, M)$ falls into one of these regions and no $\overline{X}_i$ is associated in two regions, i.e.,

$$\overline{S}_1 \cup \overline{S}_2 \cup \overline{S}_3, \ldots, \cup \overline{S}_K = \overline{S} \qquad \text{(a)}$$
$$\overline{S}_i \cap \overline{S}_j = 0 \qquad \forall\, i \neq j \qquad \text{(b)} \tag{1}$$

The K-means algorithm is based on minimization of the sum of squared distances from all points in a cluster domain to the cluster center [47]

$$\min \sum_{X \in S_j(k)} (\overline{X} - \overline{Z}_j)^2 \tag{2}$$

where $S_j(k)$ was the cluster domain for cluster centers $\overline{Z}_j$ at the k^{th} iteration, and $\overline{X}$ was a point in the cluster domain.

The cluster regions $\overline{S}_i$ represented by the cluster centers $\overline{Z}_j$, defined typical signatures or codewordd (pronunciations in the human language realm) associated with a specific state (e.g., CL, OP, PS, etc.—Table II). The number of clusters identified in each type of state was based upon the squared error distortion criterion (3). As the number of clusters increased, the distortion decreased exponentially. Following this behavior, the number of clusters was constantly increased until the squared error distortion gradient as a function of k decreased below a threshold of 1% that results in at least 10 cluster centers for 14 out of the 15 states. Selecting the most frequent 10 clusters for each state would guarantee that the squared error distortion gradient is 1% or smaller

$$d(\overline{X}, \overline{Z}) = ||\overline{X} - \overline{Z}_j||^2 = \sum_{i=1}^{k} (\overline{X} - \overline{Z}_i)^2. \tag{3}$$

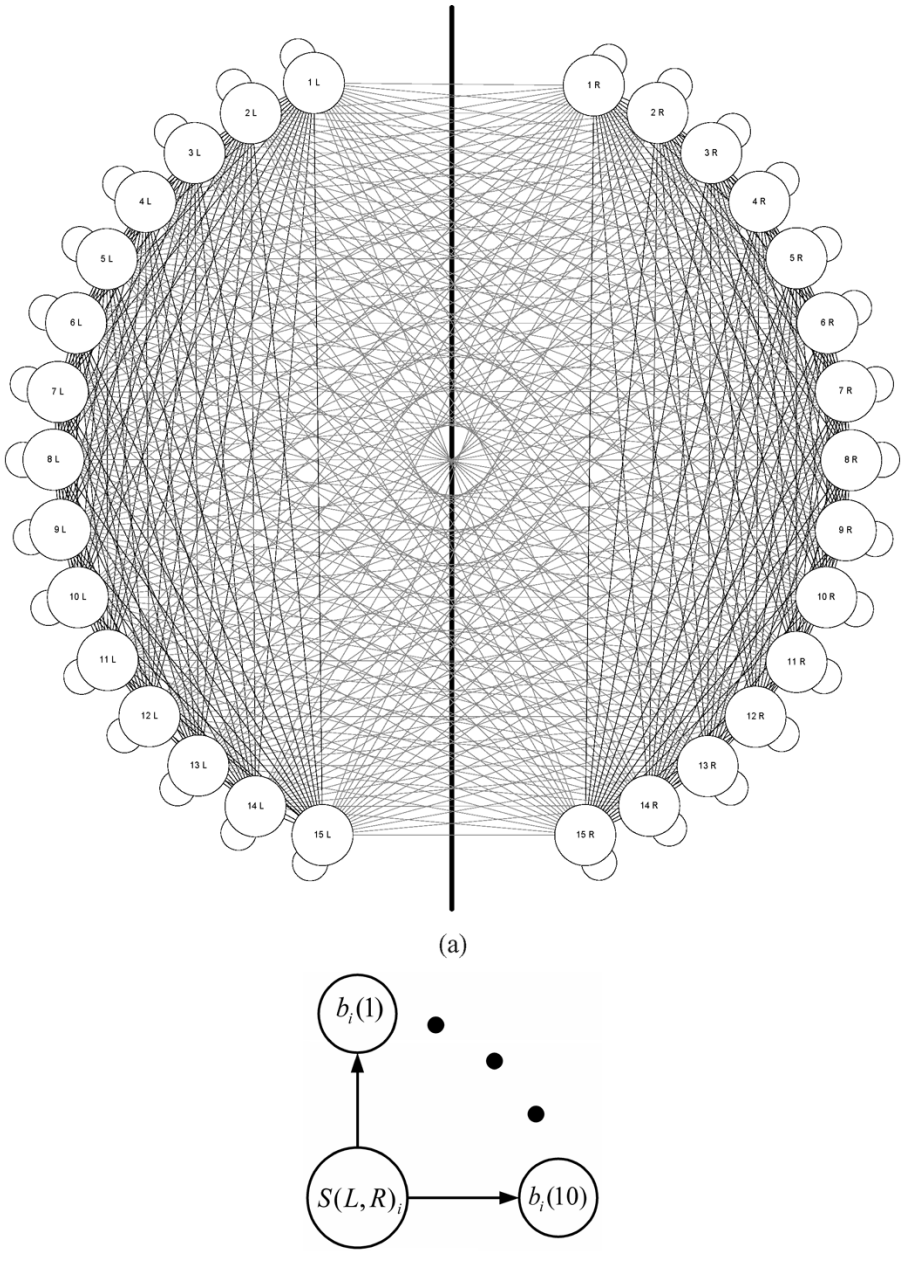

Fig. 4. FSD. (a) Fully connected FSD for decomposing MIS. The tool/tissue and tool/object interactions of the left and the right endoscopic tools are represented by the 15 fully connected submodels. Circles represent states whereas lines represent transitions between states. (b) State submodel representing the 10 discrete observation associated with it.

In the third phase, the 10 cluster centers $\overline{Z}_j$ for each state (Table II) forming a codebook of 150 discrete symbols were then used to encode the entire database of the actual surgical tasks, converting the continuous multidimensional data into a 1-D vector of finite symbols. This step of the data analysis was essential for using the discrete version of MM.

3) Markov Model (MM): The final step of the data analysis was to develop a model that represented the process of performing MIS along with the methodology for objectively evaluating surgical skill. The MM was found to be a very compact statistical method to summarize a relatively complex task, such as a step or a task of a MIS procedure. Moreover, skill level was incorporated into the MM by developing different MMs based on data acquired for different levels of expertise starting from first year residents up to expert surgeons.

The modeling approach underling the methodology for decomposing and statistically representing a surgical task is based on a fully connected, symmetric 30 state MM where the left and the right tools are represented by 15 states each (Fig. 4).

In view of this model, any MIS task may be described as a series of states. In each state, the surgeon is applying a specific force/torque/velocity signature, out of 10 signatures that are associated with that state, on the tissue or on any other item in the surgical scene by using the tool. The surgeon may stay within the same state for a specific time duration using different signatures associated with that state then perform a transition to another state. The surgeon may utilize any of the 15 states by using the left and the right tools independently. However, the states representing tool/tissue or tool/object interactions of the left and right tools are mathematically and functionally linked.

The MM is defined by the compact notation in (4). Each Markov submodel representing the left and the right tool is defined by λ_L and λ_R (4). The submodel is defined by: a) The number of states—N whereas individual states are denoted as $S = \{s_1, s_1, \ldots, s_N\}$, and the state at time t as q_t; b) The number of distinct (discrete) observation symbols—M whereas individual symbols are denoted as $V = \{v_1, v_1, \ldots, v_M\}$; c) The state transition probability distribution matrix indicating the probability of the transition from state $q_t = s_i$ at time t to state $q_{t+1} = s_j$ at time $t+1$—$A = \{a_{ij}\}$, where $a_{ij} = P[q_{t+1} = s_j | q_t = s_i]$ $1 \le i, j \le N$; Note that $A = \{a_{ij}\}$ is a nonsymmetric matrix ($a_{ij} \neq a_{ji}$) since the probability of performing a transition from state i to state j using each one of the tools is different from the probability of performing a transition from state j to state i. d) The observation symbol probability distribution matrix indicating the probability of using the symbol v_k while staying at state s_j at time t—$B = \{b_j(k)\}$, where for state j $b_j(k) = P[v_k \text{ at } t | q_t = s_j]$ $1 \le j \le N$, $1 \le k \le M$; e) The initial state distribution vector indicating the probability of starting the process with state s_i at time $t = 1 - \pi$ where $\pi_i = P[q_1 = s_i]$ $1 \le i \le N$.

The two submodels are linked to each other by the left-right interstate transition probability matrix (cooperation matrix) indicating the probability for staying in states s_l with the left tools s_r with the right tool at time t—$C = \{c_{lr}\}$, where $c_{lr} = P[q_{Lt} = s_l \cap q_{Rt} = s_r]$ $1 \le l, r \le N$. Note that $C = \{c_{lr}\}$ is a nonsymmetric matrix $c_{lr} \neq c_{rl}$ since it representing the combination of using two states simultaneously by the left and the right tools

$$\begin{aligned}
\lambda_L &= (A_L, B_L, \pi_L) \\
\lambda_R &= (A_R, B_R, \pi_R) \\
a_{ij} &= \frac{n(q_t = s_j | q_{t-1} = s_i)}{n} \\
b_{jk} &= \frac{m(v_k | q_t = s_j)}{m(q_t = s_j)} \\
c_{lr} &= \frac{c(q_{Lt} = s_l \cup q_{Rt} = s_r)}{n} \\
\sum_{j=1}^{N} a_{ij} &= \sum_{k=1}^{M} b_{jk} \sum_{l=1, r=1}^{l=N, r=N} c_{lr} = 1.
\end{aligned} \tag{4}$$

An element in the $[A]$ matrix is calculated as the ratio between the number of times a specific transition between state i to state j took place $n(q_t = s_j | q_{t-1} = s_i)$ and the total number of state transitions n which is also equal to the number of data points minus one. There are N numbers of potential transitions between two state and, therefore, the order of $[A]$ is N × N. The sum of each line in the $[A]$ matrix is equal to one. An element in the $[B]$ matrix is calculated as the ratio between the number of times a specific observation v_k was used while in state s_j, $m(v_k | q_t = s_j)$ and the total number of visits of state j, $m(q_t = s_j)$ which is also equal to the number of times any observation was used while visiting that state. There are N number states and M number of potential observations in each state and, therefore, the order of $[B]$ is N × M. The sum of each row in the $[B]$ matrix is equal to one. An element in the $[C]$ matrix is calculated as the ratio between the number of times the left-hand side model is in state s_l as well as the right-hand side of the model is in state s_r, $c(q_{Lt} = s_l \cap q_{Rt} = s_r)$ and the total number of state combinations observed n which is also equal to the number of data points. The sum of all elements of the $[C]$ matrix is equal to one.

The MM is presented graphically in Fig. 4 as a fully connected finite state diagram (FSD). The tool/tissue and tool/object interactions of the left and right endoscopic tools are each represented by the 15 fully connected submodels [Fig. 4(a)]. Circles represent states whereas lines represent transitions between states. Each line, that does not cross the center-line represents a probability value defined in the state transition probability distribution matrix $A = \{a_{ij}\}$. Each line that crosses the center-line represents a probability for a specific combination of the left and the right tools is defined by the interstate transition probability distribution matrix, or the cooperation matrix, $C = \{c_{lr}\}$. Each tool (left and right) can be only in one out of the 15 states. However, there are potentially 225 (15 × 15) different combinations in which the left tool is in state i and the right tool is in state j. For that reason the dimensions of the [C] matrix is 15 × 15. Note that since the probability of performing a transition from state i to state j by each one of the tools is different from the probability of performing a transition from state j to state i, these two probabilities should be represented by two parallel lines connecting state i to state j and representing the two potential transitions. For simplifying the graphical representation of $A = \{a_{ij}\}$ only one line is plotted between state i to state j. Each state out of the 15 states of the left and the right tool is associated with the 10 force/torque/velocity signatures or discrete observations $b_i(1), \ldots, b_i(10)$. Each line, that connects the state with a specific observation, represents a probability value defined in the observation symbol probability distribution matrix $B = \{b_j(k)\}$. The substructure appeared in Fig. 4(b) that is associated with each state was omitted for simplifying the state diagram Fig. 4(a).

The probability of observing the state transition sequence $Q = \{q_1, q_2, \ldots, q_T\}$ and the associated observation sequence $O = \{o_1, o_2, \ldots, o_T\}$, given the two Markov submodels ((4)) and interstate transition probability matrix, is defined by (5)

$$\begin{aligned}
&P(Q, O | \lambda_L, \lambda_R, C) \\
&\quad = \pi_{q_L} \pi_{q_R} \prod_{t=0}^{T} a_{Lq_t q_{t+1}} b_{Lq_t}(o_t) a_{Rq_t q_{t+1}} b_{Rq_t}(o_t) c_{q_{Lt} q_{Rt}}.
\end{aligned} \tag{5}$$

Since probabilities by definition have numerical values in the range of 0 to 1, for a relatively short time duration, the probability calculated by (5) converges exponentially to zero, therefore exceeding the precision range of essentially any machine. Hence, by using a logarithmic transformation, the resulting values of (5) in the range of [0 1] are mapped by (6) into $[-\infty\ 1]$

$$\begin{aligned}
&Log\left(P(Q, O | \lambda_L, \lambda_R, C)\right) \\
&\quad = Log\left(\pi_{q_L}\right) + Log\left(\pi_{q_R}\right) + \sum_{t=1}^{T} \Bigg(Log\left(a_{Lq_t q_{t+1}}\right) \\
&\qquad + Log\left(b_{Lq_t}(o_t)\right) + Log\left(a_{Rq_t q_{t+1}}\right) \\
&\qquad + Log\left(b_{Rq_t}(o_t)\right) + Log\left(c_{q_{Lt} q_{Rt}}\right) \Bigg).
\end{aligned} \tag{6}$$

Due to the nature of the process associated with surgery in which the procedure, by definition, always starts at the idle state (state 1), the initial state distribution vector is defined as follows:

$$\pi_{1L} = \pi_{1R} = 1$$
$$\pi_{iL} = \pi_{iR} = 0 \qquad 2 \le i \le N. \tag{7}$$

Once the MMs were defined for specific subjects with specific skill levels, it became possible to calculate the statistical distance factors between them. These statistical distance factors are considered to be an objective criterion for evaluating skill level if, for example, the statistical distance factor between a trainee (indicated by index T_j) and an expert (indicated by index E_i) is being calculated. This distance indicates the similarity between the performance of any two subjects under study. Given two MMs $\lambda_{Ei} = (\lambda_{LEi}, \lambda_{REi}, C_{Ei})$ (Expert) and $\lambda_{Ti} = (\lambda_{LTj}, \lambda_{RTj}, C_{Tj})$ (Trainee) the asymmetric statistical distances between them are defined as $D_1(\lambda_{Tj}, \lambda_{Ei})$ and $D_2(\lambda_{Ei}, \lambda_{Tj})$. The natural expression of the symmetric statistical distance version D_{EiTi} is defined by (8), shown at the bottom of the page.

Setting an expert level as the reference level of performance, the symmetric statistical distance of a model representing a given subject from a given expert (D_{EiTj}) is normalized with respect to the average distance between the models representing all the experts associated with the expert group $(\overline{D}_{EE})$—(9). The normalized distance $||D_{EiTj}||$ represents how far (statistically) is the performance of a subject, given his or her model, from the performance of the average expert

$$||D_{EiTj}|| = \frac{D_{EiTj}}{\overline{D}_{EE}} = \frac{D_{EiTj}}{\frac{1}{l}\sum_{u=1;v=1}^{u=5;v=5} D_{E_uE_v}} \qquad for\ u \ne v. \tag{9}$$

For the purpose of calculating the normalized learning curve, the 20 distances between all the expert subjects was first calculated $D_{E_uE_v}$—(for five subjects in the expert group—$u = v = 1, \ldots, 5$—$l = 20$) using (8). The denominator of (9) was then calculated. Once the reference level of expertise was determined, the statistical distances between each one of the 25 subjects, grouped into five levels of training (R1, R2, R3, R4, R5), and each one of the experts was calculated (5 distances for each individual, 25 distances for each group of skill level and 125 distances for the entire database) using (8). The average statistical distance and its variance define the learning curve of a particular task.

4) Complimentary Objective Indexes: In addition to the MMs and the statistical similarity analysis, two other objective indices of performance were measured and calculated, including task completion time and the overall path length (L) of the left and the right tool tips—(10).

$$L = \sum_{t=1}^{T} d_L\left(P_L(t-1), P_L(t)\right) + d_R\left(P_R(t-1), P_R(t)\right). \tag{10}$$

where d_L and d_R are the distances between two consecutive tool tip positions $P_L(t-1)$, $P_R(t-1)$ and $P_L(t)$, $P_R(t)$ as a function of time of the left and the right tools, respectively

D. Subjective Analysis—Scoring

The subjective performance analysis was based on an off-line unbiased expert surgeon review (blinded to the subject and training level of each individual) of digital videos recorded during the experiment. The review utilized a scoring system of 4 equally weighted criteria: (a) overall performance; (b) economy of movement; (c) tissue handling; and (d) number of errors including dropped needles, dropped sutures, lose suture loops, breaking sutures, needle injury to adjacent tissue, and inability to puncture bowel with needle. Criteria (a), (b), and (c) included 5 levels. The final scores were normalized to the averaged experts scoring.

III. Results

A. Force and Torque Position and Orientation

Typical raw data of forces and torques (F/T) and tool tip positions were plotted using 3-D graphs. The graphs show the kinematics and dynamics of the left and right endoscopic tools as measured by the Blue DRAGON while performing MIS intracorporeal knot by junior trainee [R1—Fig. 5(a), (c)] and expert surgeon [E—Fig. 5(b), (d)]. The F/T vectors can be depicted as arrows with origins located at the port, changing their lengths and orientations as a function of time as a result of the F/T applied by the surgeon's hand on the tool. In a similar fashion, the traces of the tool tips with respect to the ports were plotted in Fig. 5(c), (d) as their positions changed during the surgical procedure.

The forces along the Z axis (in/out of the port) were higher compared to the forces in the XY plane. On the other hand, torques developed by rotating the tool around the Z axis were extremely low compared to the torques generated while rotating the tool about the X and Y axes while sweeping the tissue or performing lateral retraction.

The results depicted in Fig. 5 indicate that higher forces were applied and larger workspaces were used by a trainee compared to an expert while performing the task under study. Moreover, these raw data plots demonstrate the complexity of the surgical task and the multidimensional data associated with it. This complexity can be resolved in part by decomposing the surgical task into its primary elements enabling profound understanding of the MIS task.

B. Cluster Centers and Markov Models

A cluster analysis using the K-means algorithm was performed to define typical cluster centers in the database. These were further used as code-words in the MM analysis. A total of 150 cluster centers were identified, ten clusters centers for each type of tool/tissue/object interaction as defined in

$$D_{EiTj} = \frac{D_1(O_{Ei}, Q_{Ei}, O_{Tj}, Q_{Tj}, \lambda_{Ei}) + D_2(O_{Ei}, Q_{Ei}, O_{Tj}, Q_{Tj}, \lambda_{Tj})}{2} = \frac{1}{2}\left(\frac{\log P(O_{Tj}, Q_{Tj}|\lambda_{Ei})}{\log P(O_{Ei}, Q_{Ei}|\lambda_{Ei})} + \frac{\log P(O_{Tj}, Q_{Tj}|\lambda_{Tj})}{\log P(O_{Ei}, Q_{Ei}|\lambda_{Tj})}\right) \tag{8}$$

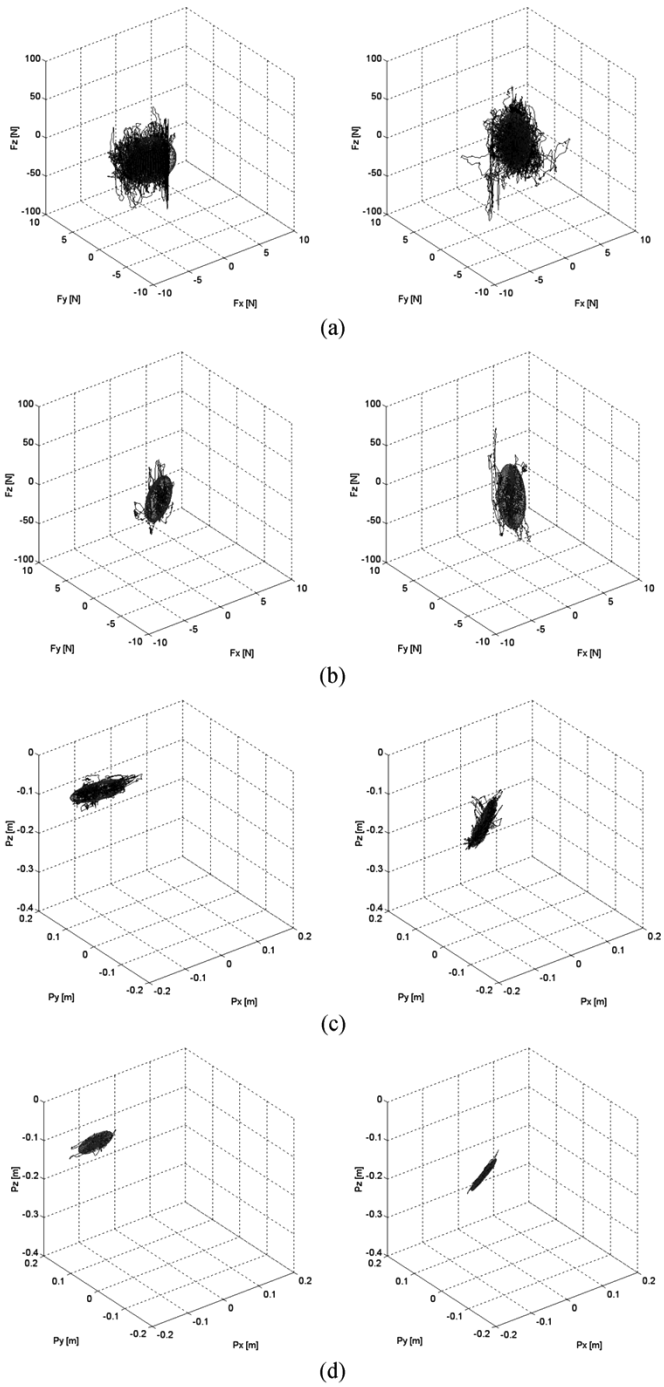

Fig. 5. Kinematics and dynamic data from left and the right endoscopic tools measured by the Blue DRAGON while performing MIS suturing and knot tying by a trainee surgeon (a),(c) and an expert surgeon (b),(d)–(a),(b) forces; (c),(d) tool tip position. The ellipsoids contain 95% of the data points.

Table II. Fig. 6 depicts the 10 cluster centers associated with each one of the 15 states identified in the data. For example, Fig. 6 (13) represents 10 cluster centers associated with the state defined by Grasping-Pushing-Sweeping (Table II—State no. 13). Grasping-Pushing-Sweeping is a superposition of three actions. The surgeon grasps a tissue or an object that is identified by the positive grasping force (F_g) acting on the tool's jaws and the negative angular velocity of the handle (ω_g) indicating that the handle is being closed. At the same time the grasped tissue or object is pushed into the port indicated by positive value of the force (F_z) acting along the long shaft of the tool and negative linear velocity (V_r) representing the fact the tool is moved into the port. Simultaneously, sweeping the tissue to the side manifested by the force and the torque in the XY plane (F_{xy}, T_{xy}) that are generated due to the deflection of the abdominal wall, the lateral force applied on the tool by the tissue or object being swept along with the lateral angular velocity (ω_{xy}) indicating the rotation of the tool around the pivot point inside the port.

Both static, quasistatic and dynamic tool/tissue or tool/ object interactions are represented by the various cluster centers. Even in static conditions, the forces and torques provide a unique and un-ambivalent signature that can be associated with each one of the 15 states. Detailed optimization analysis of the cluster centers was summarized in [25]

C. Objective and Subjective Indexes of Performance

Given the encoded data, 30 MM (one for each subject) were calculated defining the probabilities for performing certain tool transitions ($[\boldsymbol{A}]$ matrix), the probability of combining two states ($[\boldsymbol{C}]$ matrix), and the probability of using the various signatures in each state ($[\boldsymbol{B}]$ matrix)—Fig. 7. The highest probability values in the $[\boldsymbol{A}]$ matrix usually appeared along the diagonal. These results indicate that a transition associated with staying at the same state is more likely to occur rather than a transition to any one of the other 15 potential states. In MIS suturing, the default transition between any state is to the grasping state (state number 2) as indicated by the high probability values along the second column of the $[\boldsymbol{A}]$ matrix. Probability of using one out of the 150 cluster centers defined in Fig. 7 is graphically represented by the $[\boldsymbol{B}]$ matrix. Each line of the $[\boldsymbol{B}]$ matrix is associated with one of the 10 states. The clusters were ranked according to the mechanical power. The left and the right tool used different distribution of the clusters. Whereas with the left tool the most frequent clusters that were used are related to mid-range power with the right tool the cluster usage is more evenly distributed among the different power levels. The cooperation matrix $[\boldsymbol{C}]$ indicates that the most frequently used state with both the left and the right tools are idle (state 1), grasping (state 2), grasping pulling and sweeping (state 12), and grasping rotating (state 15) with the left tool. Once one of the tools utilizes one of these states, the probability of using any of the states by the other tool is equally distributed between the states which are indicated by the bright horizontal stripes in the graphical representation of the $[\boldsymbol{C}]$ matrix.

The Idle state (state 1), in which no tool/tissue (or other element) interaction is performed, was mainly used by both expert and novice surgeons, to move from one operative state to the another. However, the expert surgeons used the idle state only as a transition state while the novices spent a significant amount of time in this state planning the next tool/tissue or tool/object interaction. In the case of surgical suturing and knot tying, the grasping state (state 2) dominated the transition phases since the grasping state maintained the operative state in which both the suture and the needle were held by the two surgical tools.

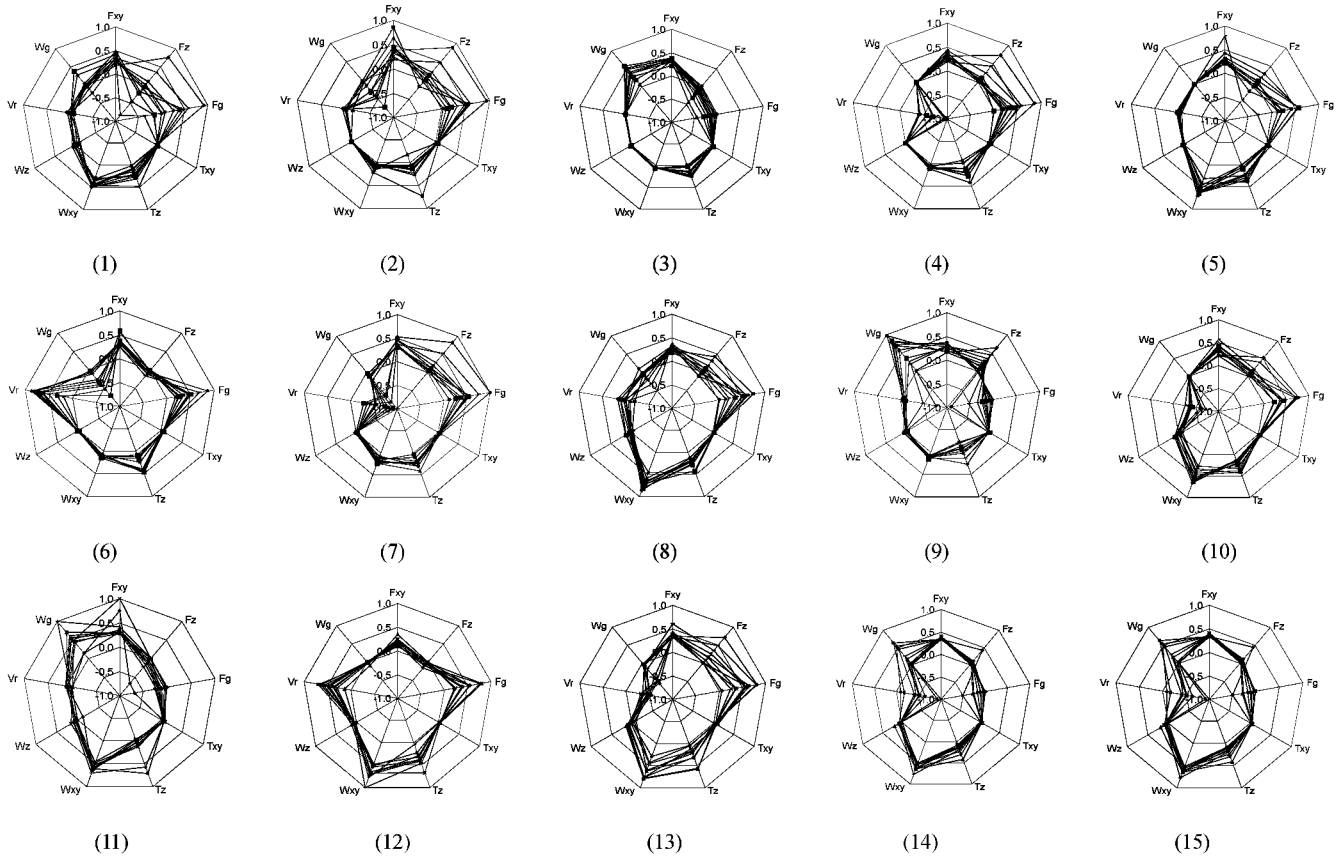

Fig. 6. Cluster centers definition—ten signatures of forces torques linear and angular velocities associated with the 15 types of states (tool/tissue or tool/object interaction) defined by Table I. In these graphs each one of the 10 polar lines represent one cluster. The clusters were normalized to a range of $[-1\ 1]$ using the following min/max values: $\omega_{xy} = 0.593$ [r/s], $\omega_Z = 2.310$ [r/s], $V_r = 0.059$ [m/s], $\omega_g = 0.532$ [r/s], $F_{xy} = 5.069$ [N], $F_Z = 152.536$ [N], $F_g = 33.669$ [N], $T_{xy} = 9.792$ [Nm], and $T_Z = 0.017$ [Nm]. The numbers correspond to the 15 states as defined by Table I.

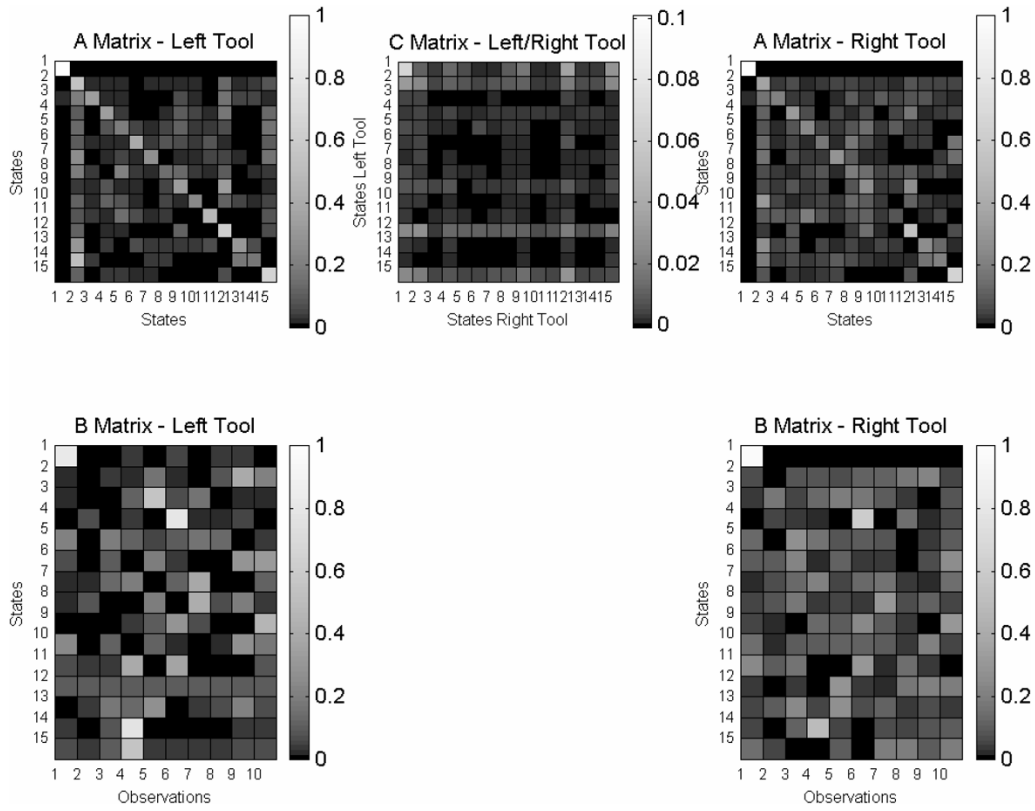

Fig. 7. A typical MM where the matrices $[\boldsymbol{A}]$, $[\boldsymbol{B}]$, $[\boldsymbol{C}]$, are represented as color-coded probabilistic maps.

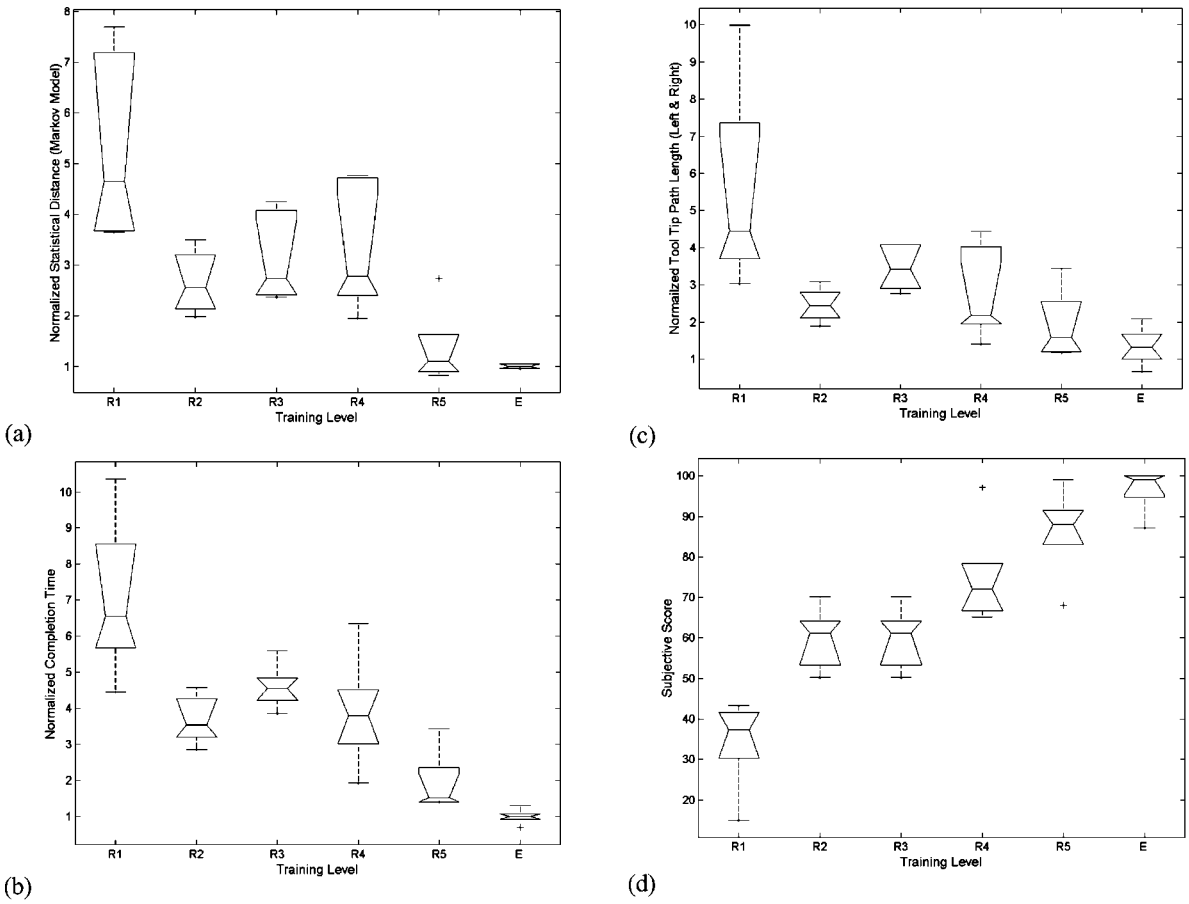

Fig. 8. Objective and subjective assessment indexes of minimally invasive suturing learning cure. The objective performance indexes are based on: (a) MM normalized statistical distance, (b) normalized completion time, and (c) normalized path length of the two tool tips. The average task completion time of the expert group is 98 sec and the total path length of the two tools is 3.832 m. The subjective performance index is based on visual scoring by an expert surgeon normalized with respect to experts' performance (d).

Fig. 8(a)–(c) represents the normalized MM-based statistical distance as a function of the training level, the normalized completion time, and the normalized path length of the two tool tips, respectively. The subjective normalized scoring is depicted in Fig. 8(d). The data demonstrate that substantial suturing skills are acquired during the first year of the residency training. The learning curves do not indicate any significant improvement during the second and the third years of training. The rapid improvement of the first year is followed by a lower gradient of the learning curve as the trainees progress toward the expert level. However, the MM based statistical distance [Fig. 8(a)] along with the completion time criteria [Fig. 8(b)] show yet another gradient in the learning curve that occurs during the fourth year of the residency training followed by slow conversion to expert performance. Similar trends in the learning curve are also demonstrated by the subjective assessment [Fig. 8(d)]. One of the subjects in the R2 group outperformed his peers in his own group and some subjects in more advanced groups (R3, R4). Although statistically insignificant, the performance slightly altered the overall trend of the learning curves as defined by the different criteria.

A correlation analysis was performed between the means of the objective normalized MM based statistical distance and the subjective normalized scoring (Fig. 9). The value of the correlation factor (R^2) was found to be 0.86 indicating a significant correlation $(\mathrm{p} < 0.05)$ between the MM objective evaluation and the subjective skill evaluation method. This result suggests that 86% of the objective MM skill evaluation variance is attributed to linear covariance of the subjective skill evaluation while 14% of the of the objective MM skill evaluation variance is unexplained by the subjective skill evaluation.

Detailed analysis of the MM shows that major differences between surgeons at different skill levels were: 1) the types of tool/tissue/object interactions being used; 2) the transitions between tool/tissue/object interactions being applied by each hand; 3) time spent while performing each tool/tissue/object interaction; 4) the overall completion time; 5) the various F/T/velocity magnitudes being applied by the subjects through the endoscopic tools; 6) two-handed collaboration. Moreover, high efficiency of surgical performance was demonstrated by the expert surgeons and expressed by shorter tool tip displacements, shorter periods of time spent in the "idle" state, and sufficient application of F/T on the tissue to safely accomplish the task.

IV. Discussion

Minimally invasive surgery, regardless of the modality being used, is a complex task that requires synthesis between visual and kinesthetic information. Analyzing MIS in terms of these two sources of information is a key step toward developing objective criteria for training surgeons and evaluating their performance in different modalities including real surgery,

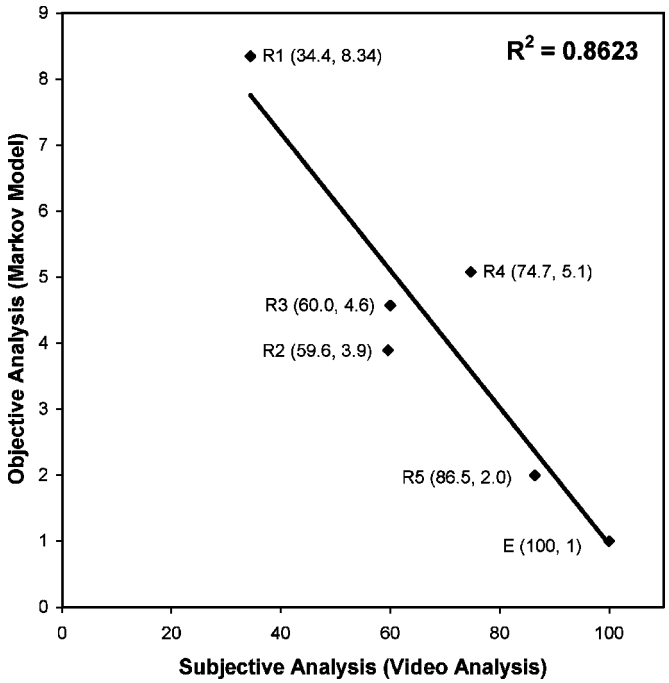

Fig. 9. Linear correlation between the normalized mean performance obtained by a subjective video analysis and objective analysis using MMs and the statistical distance between models of trainees (R1–R5) and experts (E). The notations R1, R2, R3, R4, and R5 represent the various residence groups where the number denotes year of training and E indicate expert surgeons. The values in the brackets represent the normalized mean scores using the subjective and the objective methodologies, respectively.

master/slave robotic systems or virtual reality simulators with haptic technology.

Following two steps of data reduction that were collected by the Blue DRAGON were further used to develop models representing MIS as a process. In any data reduction there is always a compromise between decreasing the input dimensionality and retaining sufficient information to characterize and model the process under study. Utilizing the VQ algorithm the 13-D stream of acquired data was quantized into 150 symbols with nine dimensions each.

The data quantization included two substeps. In the first steps the cluster centers were identified. As part of the second step the entire database was encoded based on the cluster centers defined in the first step. Every data point needs to meet two criteria in order to be associated with one of the 150 cluster centers defined in the first step. The first criterion is to have the minimal geometrical distance to one of the cluster centers. Once the data point was associated with a specific cluster center it is by definition associated with a specific state out the 15 defined. Based on expert knowledge of surgery, Table II defines the 15 states and unique sets of individual vector components. The second criterion is that given the candidate state and the data vector, the direction of each component in the vector must match the one defined by the table for the selected state. It was indicated during the data processing that these two criteria were always met suggesting that the data quantization process is very robust in its nature. Following the encoding process a two-dimensional input (one dimension for each tool) was utilized to form a 30 state fully connected MM. The coded data with their close association to the measured data, as well as the MM using these codes as its observations distributed among its states, retain sufficient multi model information in a compact mathematical formulation for modeling the process of surgery at different levels.

MIS is recognized both qualitatively and quantitatively as a multidimensional process. As such, studying one parameter, e.g., completion time, tool-tip paths, or force/torque magnitudes reveals only one aspect of the process. Only a model that truly describes MIS as a process is capable of exposing the internal process and provide a wide spectrum of information about it. At the high level, a tremendous amount of information is encapsulated into a single objective indicator of surgical skill level and expressed as the statistical distance between the surgical performance of a particular subject under study from the surgical performance of an expert. As part of an alternative approach a combined score could be calculated by studying each parameter individually (e.g., force, torque, velocity, tool path, completion time, etc.), assigning a weight to each one of these parameters, which is a subjective process by itself, and combining them into a single score. The assumption underlying this approach is that a collection of aspects associated with surgery may be used to assess the overall process. However, this alternative approach ignores the internal process that is more likely to be revealed by a model such as the MM. In addition, as opposed to analyzing individual parameters, studying the low levels of the model provides profound insight into the process of MIS in a way that allows one to offer constructive feedback for a trainee regarding various performance aspects such as the appropriate application of F/T, economy of motion, and two-handed manipulation.

The appropriate application of F/T on the tissue has a significant impact on the surgical performance efficiency and outcome of surgery. Previous results indicated that the F/T magnitudes are task dependent [3]–[6]. Experts applied high F/T magnitudes on the tissues during tissue dissection as opposed to low F/T magnitudes applied on the tissues by trainees that were trying to avoid irreversible damage. An inverse relationship regarding the F/T magnitudes was observed during tissue manipulation in which high F/T magnitudes applied on the tissue by trainees exposed them to acute damage. It is important to point out that these differences were observed in particular states (e.g all the states including grasping for tissue manipulation and all the state that involved spreading for tissue dissection). Due to the inherent variance in the data even multidimensional analysis of variance failed to identify this phenomena once the F/T magnitudes are removed from the context of the multi state model. Given the nature of surgical task, the MM [B] Matrix, encompassing information regarding the frequency in which the F/T magnitudes were applied, may be used to assess whether the appropriate magnitudes F/T were applied for each particular state. For obvious reasons, tissue damage is correlated with surgical outcome, and linked to the magnitudes and the directions in which F/T were applied on the tissues. As such, tissue damage boundaries may be incorporated into the [B] matrix for each particular state. Given the surgical task, this additional information may refine the constructive feedback to the trainee and the objective assessment of the performance.

The economy of motion and the two-hand collaboration may be further assessed by retrieving the information encapsulated

into the [A] and [C] matrices. The amount of information incorporated into these two data structures is well beyond the information provided by a single indicator such as tool-tip path length, or completion time for the purpose of formulating constructive feedback to the trainee. Given a surgical task, utilizing the appropriate sets of states and state transitions are skill dependent. This information is encompassed in the [A] matrix indicating that the states that were in use and the state transitions that were performed. Moreover, the ability to refine the time domain analysis using the multi state MM indicated, as was observed in previous studies, that the "idle" state is utilized as a transition state by expert surgeons whereas a significant amount of time is spent in that state by trainees [3]–[6]. In addition, coordinated movements of the two tools is yet another indication of high skill level of MIS. At a lower skill level the dominant hand is more active than the nondominant hand as opposed to a high skill level in which the two tools are utilized equally. The collaborated [C] matrix encapsulates this information and quantifies the level of collaboration between the tools.

In conclusion, the MM provides insight into the process of performing MIS. This information can be translated into constructive feedback to the trainee as indicated by the model's three matrices [A], [B], and [C]. Moreover, the capability of running the model in real time and its inherent memory allows a senior surgeon supervising the surgery or an artificial intelligent expert system incorporated into a surgical robot or a simulator to provide immediate constructive feedback during the process as previously described.

A useful analogy of the proposed methodology for decomposing the surgical task is the human spoken language. Based on this analogy, the basic states—tool/tissue interactions are equivalent to "words" of the MIS "language" and the 15 states form the MIS "dictionary" or set of all available words. In the same way that a single word can be pronounced differently by various people, the same tool/tissue or tool/object interaction can be performed differently by different surgeons. Differences in F/T magnitudes account for this different "pronunciation," yet different pronunciations of a "word" have the same meaning, or outcome, as in the realm of surgery. The cluster analysis was used to identify the typical F/T and velocities associated with each one of the tool/tissue and tool/object interactions in the surgery "dictionary," or using the language analogy, to characterize different pronunciations of a "word." Utilizing the "dictionary" of surgery, the MM was then used to define the process of each task or step of the surgical procedure, or in other words, "dictating chapters" of the surgical "story." This analogy is reinforced by an important finding in the field of Phonology suggesting that all human languages use a limited repertoire of about 40 to 50 sounds defined as phones [26], e.g., the DARPA phonetic alphabet, ARPAbet, used in American English or the International Phonetic Alphabet. The proposed methodology retains its power by decomposing the surgical task to its fundamental elements—tool/tissue and tool/object interactions. These elements are inherent in MIS no matter which modality is being used.

One may note that although the notations and the model architecture of the proposed MM and the HMM approach are similar, there are several fundamental differences between them. Strictly speaking, the proposed MM is a white box model in which each state has a physical meaning describing a particular interaction between the tools and tissue or other objects in the surgical scene like sutures and needles. However, the HMM is a black box model in which the states are abstract and are not related to a specific physical interaction. Moreover, in the proposed white box model, each state has a unique set of observations that characterize only the specific state. By definition, once the discrete observation is matched with a vector quantization code-word the state is also defined. States in the HMM share the same observations, however different observation distributions differentiate between them. The topology of the proposed MM suggests a hybrid approach between the two previously described models. It adds to the classic MM another layer of complexity by introducing the observation elements for each state. The model also provides insight into the process by linking the states to physical and meaningful interactions. This unique quality adds to the classic notation the introduction of the cooperation matrix [C]. This matrix is not present in either the MM or the HMM. The [C] matrix was introduced as a way to link between the models representing the left- and right-hand tools since surgery is a two-handed task.

Quantifying the advantages and the disadvantages of each modeling approach (MM or HMM) is still a subject for active research. Whereas the strength of the MM is expressed by providing physical meaning to the process being modeled, development of HMM holds the promise for more compact model topology which avoids any expert knowledge incorporated into the model. Regardless of the type of the model, defining the scope of the model and its fundamental elements, the state and the observation are subjects of extensive research. In the current study the entire surgical task is modeled by a fully connected model topology were each tool/tissue/object interaction is modeled as a state. In a different approach, using a state of the art methodology in speech recognition in which each phenomenon is represented by a model with abstract states, each tool/object interaction is modeled by entire model using more generalized definitions for these interactions, e.g., place position, insert remove [27], [28]. This approach may require an additional model with a predetermined overall structure that will represent the overall process.

The scope of the proposed model is limited to objectively assess technical factors of surgical ability. Cognitive factors per se cannot be assessed by the model unless a specific action is taken as a result of a decision making process. In any case, the model is incapable of tracing the process back to its cognitive origin. In addition, the underlying assumption made by using a model is that there is a standard technique with insignificant variations by which expert surgeons perform a surgical task. Any significant variation of the surgical performance, regardless of the surgical outcome, is penalized by the model and associated with low scores. If such a surgical performance variation from the standard surgical technique is associated with a better outcome for the patient the model is incapable of detecting it.

Decomposing MIS and analyzing it using MM is one approach for developing objective criteria for surgical performance. The availability of validated objective measures of

surgical performance and competency is considered critical for training surgeons and evaluating their performance. Systems like surgical robots or virtual reality simulators that inherently measure the kinematics and the dynamics of the surgical tools may benefit from inclusion of the proposed methodology. Using this information in real time during the course of learning as feedback to the trainee surgeons or as an artificial intelligent background layer, may increase performance efficiency in MIS and improve patient safety and outcome.

REFERENCES

[1] R. Satava, "Developing Quantitative Measurements Through Surgical Simulation," presented at the Metrics for Objective Assessment of Surgical Skills Workshop, Scottsdale, AZ, Jul 2001.

[2] A. G. Gallagher and R. M. Satava, "Virtual reality as a metric for the assessment of laparoscopic psychomotor skills. Learning curves and reliability measures," *Surg Endosc.*, vol. 16, no. 12, pp. 1746–1752, Dec. 2002.

[3] J. Rosen, B. Hannaford, C. Richards, and M. Sinanan, "Markov modeling of minimally invasive surgery based on tool/tissue interaction and force/torque signatures for evaluating surgical skills," *IEEE Trans. Biomed. Eng.*, vol. 48, no. 5, pp. 579–591, May 2001.

[4] C. Richard, J. Rosen, B. Hannaford, M. MacFarlane, C. Pellegrini, and M. Sinanan, "Skills evaluation in minimally invasive surgery using force/torque signatures," *Surg. Endosc.*, vol. 14, no. 9, pp. 791–798.

[5] J. Rosen, M. Solazzo, B. Hannaford, and M. Sinanan, "Objective evaluation of laparoscopic skills based on haptic information and tool/tissue interactions," *Comput. Aided Surg.*, vol. 7, no. 1, pp. 49–61, July 2002.

[6] J. Rosen, J. D. Brown, M. Barreca, L. Chang, B. Hannaford, and M. Sinanan, "The Blue DRAGON, a system for monitoring the kinematics and the dynamics of endoscopic tools in minimally invasive surgery for objective laparoscopic skill assessment," presented at the MMVR 2002, Newport Beach, CA, 2002.

[7] J. Rosen, J. D. Brown, L. Chang, M. Barreca, M. Sinanan, and B. Hannaford, "The Blue DRAGON—a system for measuring the kinematics and the dynamics of minimally invasive surgical tools *in vivo*," presented at the IEEE Int. Conf. Robotics and Automation, Washington DC, May 11–15, 2002.

[8] P. B. McBeth, A. J. Hodgson, A. G. Nagy, and K. Qayumi, "Quantitative methodology of evaluating surgeon performance in laparoscopic surgery," presented at the MMVR 2002, Newport Beach, CA, 2002.

[9] J. A. Ibbotson, C. L. MacKenzie, C. G. L. Cao, and A. J. Lomax, "Gaze patterns in laparoscopic surgery," in *Medicine Meets Virtual Reality: 7*, J. D. Westwood, H. M. Hoffman, R. A. Robb, and D. Stredney, Eds. Washington, DC: IOS Press, 1999, pp. 154–160.

[10] C. M. Pugh and P. Youngblood, "Development and validation of assessment measures for a newly developed physical examination simulator," *J. Am. Med. Inform. Assoc.*, vol. 9, no. 5, pp. 448–460, Sep.–Oct. 2002.

[11] M. Noar, "Endoscopy simulation: a brave new world?," *Endoscopy*, vol. 23, pp. 147–149, 1991.

[12] R. Satava, "Virtual reality surgical simulator," *Surg. Endosc.*, vol. 7, pp. 203–205, 1993.

[13] D. Ota, B. Loftin, T. Saito, R. Lea, and J. Keller, "Virtual reality in surgical education," *Comput. Biol. Med.*, vol. 25, pp. 127–137, 1995.

[14] B. J. S. Weghorst, H. Gladstone, G. Raugi, and M. Ganter, "Fast finite element modeling for surgical simulation," *Student Health Technol. Inf.*, vol. 62, pp. 55–61, 1999.

[15] C. S. Tseng, Y. Y. Lee, Y. P. Chan, S. S. Wu, and A. W. Chiu, "A PC-based surgical simulator for laparoscopic surgery," *Student Health Technol. Inf.*, vol. 50, pp. 155–160, 1998.

[16] H. Delingette, S. Cotin, and N. Ayache, "Efficient linear elastic models of soft tissues for real-time surgery simulation," *Stud Health Technol. Inf.*, vol. 62, pp. 100–101, 1999.

[17] C. Basdogan, C. H. Ho, and M. A. Srinivasan, "Simulation of tissue cutting and bleeding for laparoscopic surgery using auxiliary surfaces," *Student Health Technol. Inf.*, vol. 62, pp. 38–44, 1999.

[18] E. Acosta, B. Temkin, T. M. Krummel, and W. L. Heinrichs, "G2H—graphics-to-haptic virtual environment development tool for PC's.," *Student Health Technol. Inf.*, vol. 70, pp. 1–3, 2000.

[19] Y. Akatsuka, T. Shibasaki, A. Saito, A. Kosaka, H. Matsuzaki, T. Asano, and Y. Furuhashi, "Navigation system for neurosurgery with PC platform," *Student Health Technol. Inf.*, vol. 70, pp. 10–16, 2000.

[20] J. Berkley, P. Oppenheimer, S. Weghorst, D. Berg, G. Raugi, D. Haynor, M. Ganter, C. Brooking, and G. Turkiyyah, "Creating fast finite element models from medical images," *Student Health Technol. Inf.*, vol. 70, pp. 26–32, 2000.

[21] N. El-Khalili, K. Brodlie, and D. Kessel, "WebSTer: a web-based surgical training system," *Student Health Technol. Inf.*, vol. 70, pp. 69–75, 2000.

[22] R. Friedl, M. Preisack, M. Schefer, W. Klas, J. Tremper, T. Rose, J. Bay, J. Albers, P. Engels, P. Guilliard, C. F. Vahl, and A. Hannekum, "CardioOp: an integrated approach to teleteaching in cardiac surgery," *Student Health Technol. Inf.*, vol. 70, pp. 76–82, 2000.

[23] E. Gobbetti, M. Tuveri, G. Zanetti, and A. Zorcolo, "Catheter insertion simulation with co-registered direct volume rendering and haptic feedback," *Student Health Technol. Inf.*, vol. 70, pp. 96–98, 2000.

[24] P. Gorman, T. Krummel, R. Webster, M. Smith, and D. Hutchens, "A prototype haptic lumbar puncture simulator," *Student Health Technol. Inf.*, vol. 70, pp. 106–109, 2000.

[25] J. Anne-Claire, Q. Denis, D. Patrick, C. Christophe, M. Philippe, K. Sylvain, and G. Carmen, "S.P.I.C. pedagogical simulator for gynecologic laparoscopy," *Student Health Technol. Inf.*, vol. 70, pp. 139–145, 2000.

[26] J. L. Tasto, K. Verstreken, J. M. Brown, and J. J. Bauer, "PreOp endoscopy simulator: from bronchoscopy to ureteroscopy," *Student Health Technol. Inf.*, vol. 70, pp. 334–349, 2000.

[27] G. J. Wiet, D. Stredney, D. Sessanna, J. A. Bryan, D. B. Welling, and P. Schmalbrock, "Virtual temporal bone dissection: an interactive surgical simulator," *Otolaryngol Head Neck Surg.*, vol. 127, no. 1, pp. 79–83, Jul. 2002.

[28] N. W. John, N. Thacker, M. Pokric, A. Jackson, G. Zanetti, E. Gobbetti, A. Giachetti, R. J. Stone, J. Campos, A. Emmen, A. Schwerdtner, E. Neri, S. S. Franceschini, and F. Rubio, "An integrated simulator for surgery of the petrous bone," *Student Health Technol. Inf.*, vol. 81, pp. 218–224, 2001.

[29] D. Berg, J. Berkley, S. Weghorst, G. Raugi, G. Turkiyyah, M. Ganter, F. Quintanilla, and P. Oppenheimer, "Issues in validation of a dermatologic surgery simulator," *Student Health Technol. Inf.*, vol. 81, pp. 60–65, 2001.

[30] M. J. Manyak, K. Santangelo, J. Hahn, R. Kaufman, T. Carleton, X. C. Hua XC, and R. J. Walsh, "Virtual reality surgical simulation for lower urinary tract endoscopy and procedures," *J. Endourol.*, vol. 16, no. 3, pp. 185–90,, Apr. 2002.

[31] C. Basdogan, C. Ho, and M. A. Srinivasan, "Virtual environments for medical training: graphical and haptic simulation of common bile duct exploration (PDF)," *IEEE/ASME Trans. Mechatronics (Special Issue on Haptic Displays and Applications)*, vol. 6, no. 3, pp. 267–285, Sep. 2001.

[32] C. G. L. Cao, C. L. MacKenzie, J. A. Ibbotson, L. J. Turner, N. P. Blair, and A. G. Nagy, "Hierarchical decomposition of laparoscopic procedures," in *Medicine Meets Virtual Reality: 7*, J. D. Westwood, H. M. Hoffman, R. A. Robb, and D. Stredney, Eds. Washington, DC: IOS Press, 1999, pp. 83–89.

[33] M. C. Cavusoglu, I. Villanueva, and F. Tendick, "Workspace analysis of robotic manipulator for teleoperated suturing task," presented at the IEEE/IROS Conf., Maui, HI, 2001.

[34] L. R. Rabiner, "A tutorial on hidden Markov models and selected application in speech recognition," *Proc. IEEE*, vol. 77, no. 2, Feb. 1989.

[35] B. Hannaford and P. Lee, "Hidden Markov model of force torque information in telemanipulation," *Int. J. Robot. Res.*, vol. 10, no. 5, pp. 528–539, 1991.

[36] P. Pook and D. H. Ballard, "Recognizing teleoperated manipulations," in *Proc. IEEE Robotics and Automation Conf.* , vol. 2, Atlanta, GA, May 1993, pp. 578–585.

[37] M. C. Nechyba and Y. Xu, "Stochastic similarity for validating human control strategy models," *IEEE Trans. Robot. Automat.*, vol. 14, no. 3, pp. 437–451, Jun. 1998.

[38] J. Yang, Y. Xu, and C. S. Chen, "Human action learning via hidden Markov model," *IEEE Trans. Syst., Man, Cybern., Part A (Systems & Humans)*, vol. 27, no. 1, pp. 34–44, Jan. 1997.

[39] K. Itabashi, K. Hirana, T. Suzuki, S. Okuma, and F. Fujiwara, "Modeling and realization of the peg-in-hole task based on hidden Markov model," in *Proc. IEEE Int. Conf. Robotics and Automation*, Leuven, Belgium, May 1998, p. 1142.

[40] "Gesture and sign language in human-computer interaction," presented at the Gesture Workshop, I. Wachsmuth and M. Frohlich, Eds., Berlin, Germany, 1998.

[41] J. J. Lien, T. Kanade, J.-F. Cohn, and L. Ching-Chung, "Automated facial expression recognition based on FACS action units," in *Proc. 3rd IEEE Int. Conf. Automatic Face and Gesture Recognition (Cat. no. 98EX107)*, Nara, Japan, Apr. 14–16, 1998, pp. 390–395.

[42] P. Baldi and S. Brunak, *Bioinformatics*. Cambridge: MIT Press, 1998.
[43] T. E. Murphy, C. M. Vignes, D. D. Yuh, and A. M. Okamura, "Automatic motion recognition and skill evaluation for dynamic tasks," in *Eurohaptics*, 2003, pp. 363–373.
[44] S. J. Russell and P. Norvig, *Artificial Intelligence—A Modern Approach*, 2nd ed. Upper Saddle River, NJ: Pearson Education, 2003.
[45] M. Li and A. M. Okamura, "Recognition of operator motions for real-time assistance using virtual fixtures," in *Proc. 11th Int. Symp. Haptic Interfaces for Virtual Environment and Teleoperator Systems, IEEE Virtual Reality*, 2003, pp. 125–131.
[46] C. S. Hundtofte, G. D. Hager, and A. M. Okamura, "Building a task language for segmentation and recognition of user input to cooperative manipulation systems," in *Proc. 10th Int. Symp. Haptic Interfaces for Virtual Environment and Teleoperator Systems*, 2002, pp. 225–230.
[47] S. T. Bow, *Pattern Recognition*. New York: Marcel, Dekker Inc., 1984.

Jacob Rosen (M'01) received the B.Sc. degree in mechanical engineering and the M.Sc. and Ph.D. degrees in biomedical engineering from Tel-Aviv University, Tel-Aviv, Israel, in 1987, 1993, and 1997, respectively.

From 1987 to 1992, he served as an Officer in the IDF studying human-machine interfaces. From 1993 to 1997, he was a Research Associate developing and studying the EMG based powered Exoskeleton at the Biomechanics Laboratory, Department of Biomedical Engineering, Tel-Aviv University. During the same period of time he held a biomechanical engineering position in a startup company developing innovative orthopedic spine/pelvis implants. Since 1997, he has been at the University of Washington, Seattle, with an appointment of Research Assistant Professor of Electrical Engineering since 2000 and an adjunct appointment with the Department of Surgery since 2002. His research interests focus on surgical robotics, biorobotics, biomechanics, and human-machine interface.

The study reported hereby was presented in part at the IEEE International Conference on robotics and Automation (ICRA), Washington D.C. May, 2002. For that contribution Dr. Rosen and the coauthors were nominated as finalist for the Wegbreit best manipulation paper award in the IEEE ICRA 2002

Jeffrey D. Brown received B.Sc. degree in in biomedical engineering form Arizona State University, Tempe, in 1997. He was awarded a Whitaker Foundation Graduate Research Fellowship to attend the University of Washington in the fall of 1998. He received the Ph.D. degree in bioengineering from the University Washington in 2003.

Lily Chang received the M.D. degree from Tufts University, Medford, MA, in 1996 and completed residency in General Surgery at the University of Washington, Seattle, in 2001.

She then pursued a fellowship in Minimally Invasive Surgery also at University of Washington and subsequently joined the faculty as an Assistant Professor. Her research interests include innovations in the field of laparoscopic surgery, clinical use of robotic surgery, surgical telementoring, and improvement of surgical training and education. She is active in the Center for Videoendoscopic Surgery training courses for community surgeons and resident education.

Dr. Chang is a member of the American College of Surgeons, Society of American Gastrointestinal and Endoscopic Surgeons, and other local societies.

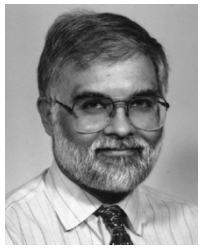

Mika N. Sinanan received the M.D. degree from Johns Hopkins University, Baltimore, MD, in 1980, and the Ph.D. degree in gastrointestinal physiology from the University of British Columbia, Vancouver, BC, Canada, in 1991.

He completed training in General and Gastrointestinal Surgery at the University of Washington (UW), Seattle, in 1988 and joined the faculty the UW. Currently, he is a Professor of Surgery and Adjunct Professor of Electrical Engineering at the University of Washington, Chief of Medical Staff and a Co-Director of the Center of Video Endoscopic Surgery. His research interests focus on technical surgical education, clinical application of advanced videoendoscopic surgical procedures, surgical robotics and Telemedicine. He is a member of the American College of Surgeons, Society for Surgery of the Alimentary Tract, Society of American Gastrointestinal and Endoscopic Surgeons, Society of Laparendoscopic Surgeons, National Cancer Committee Network, American Medical Association, American Society of Colon and Rectal Surgeons, American Society of Gastrointestinal Endoscopy, American Society of Quality, American Telemedicine Association, International Association of Pancreatology, and other regional societies.

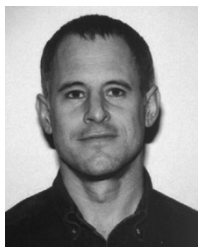

Blake Hannaford (S'82–M'85-SM'01–F'06) received the B.S. degree in engineering and applied science from Yale University, New Haven, CT, in 1977, and the M.S. and Ph.D. degrees in electrical engineering from the University of California, Berkeley, in 1982 and 1985, respectively. At Berkeley, he pursued thesis research in multiple target tracking in medical images and the control of time-optimal voluntary human movement.

Before graduate study, he held engineering positions in digital hardware and software design, office automation, and medical image processing. From 1986 to 1989, he worked on the remote control of robot manipulators in the Man-Machine Systems Group in the Automated Systems Section of the NASA Jet Propulsion Laboratory, Caltech. He supervised that group from 1988 to 1989. Since September 1989, he has been at the University of Washington, Seattle, where he has been Professor of Electrical Engineering since 1997. His currently active interests include haptic displays on the internet, surgical biomechanics, and biologically based design of robot manipulation.

Dr. Hannaford was awarded the National Science Foundation's Presidential Young Investigator Award and the Early Career Achievement Award from the IEEE Engineering in Medicine and Biology Society.